Separation Science and Technology
Publication details, including instructions for authors and subscription information:
http://www.informaworld.com/smpp/title~content=t713708471

Studies on Thermal Properties of Selected Aprotic and Protic Ionic Liquids

Huimin Luo[a]; Jing-Fang Huang[b]; Sheng Dai[b]
[a] Nuclear Science and Technology Division, [b] Chemical Sciences Division, Oak Ridge National Laboratory, Oak Ridge, TN, USA

To cite this Article Luo, Huimin , Huang, Jing-Fang and Dai, Sheng(2008) 'Studies on Thermal Properties of Selected Aprotic and Protic Ionic Liquids', Separation Science and Technology, 43: 9, 2473 — 2488
To link to this Article: DOI: 10.1080/01496390802151922
URL: http://dx.doi.org/10.1080/01496390802151922

Separation Science and Technology, 43: 2473–2488, 2008

ISSN: 0149-6395 print/1520-5754 online
DOI: 10.1080/01496390802151922

Taylor & Francis
Taylor & Francis Group

Studies on Thermal Properties of Selected Aprotic and Protic Ionic Liquids

Huimin Luo,[1] Jing-Fang Huang,[2] Sheng Dai,[2]
[1]Nuclear Science and Technology Division
[2]Chemical Sciences Division, Oak Ridge National Laboratory, Oak Ridge, TN, USA

Abstract: We describe herein the thermal gravimetric analysis (TGA) and differential scanning calorimetry (DSC) investigations of the thermal properties of selected room-temperature ionic liquids (RTILs). The dependence of the thermal properties on both cation and anion structures of RTILs was systematically studied. The ionic liquids (ILs) investigated here include 28 different imidazolium-based ILs, 22 ammonium-based ILs, and 16 amide-based ILs. In general, these three cation classes exhibit different thermal behaviors but follow a quite systematic trend as expected from the corresponding structural variation. The ILs with bromide as the conjugate anion have lower thermal stabilities than those with bis(trifluoromethane sulfonyl) imide or bis(perfluoroethyl sulfonyl) imide as the conjugate anion. The mass of TGA samples and scan rate were found to have a systematic effect on the decomposition temperature of ILs, highlighting the caution needed in reporting TGA results.

Keywords: Ionic liquids, TGA/DSCs, thermal properties

INTRODUCTION

Room-temperature ionic liquids are defined as salts that are liquid below 100°C (1,2). Many of ionic liquids, unlike conventional molecular solvents currently in use, are nonflammable, chemically tunable, and exert no detectable vapor pressure. These unique features have led to their designation as "designer solvents" for use as potential replacements for noxious volatile organic compounds (VOCs), which can contribute to air

Received 25 October 2007; accepted 3 April 2008.
Address correspondence to Huimin Luo, Nuclear Science and Technology Division, Oak Ridge National Laboratory, Oak Ridge, TN, 37831, USA. E-mail: luoh@ornl.gov.

pollution and health problems for process workers (3). Our continuing interest in the development of new solvent-extraction systems based on ILs for separation of fission products from high level wastes (4–6) prompted us to synthesize a large number of different classes of RTILs. The thermal properties of most of these RTILs with exception of few imidazolium-based ILs (7–11) have not been reported. The knowledge of the thermal properties associated with these RTILs is important in many practical applications including solvent extractions. In this paper, we describe the thermal gravimetric analysis (TGA) and differential scanning calorimetry (DSC) investigations of the thermal properties of these RTILs. The dependence of the thermal properties on both cation and anion structures of RTILs was investigated. The chemical abbreviations and structures of the investigated organic salts are illustrated in Schemes I.

A number of publications have appeared recently on the TGA and DSC investigations of imidazolium-based ILs. Notably, Ngo et al. have showed a strong dependence of decomposition temperature of ILs on both cation and anion structures (8). Wilkes and his coworkers have systematically investigated the thermal stabilities and conductivities of a number of imidazolium-based ILs for their potential applications in heat-transfer fluids (11). Brennecke and coworkers have conducted the measurement of thermal properties of selected aprotic ILs in relation to

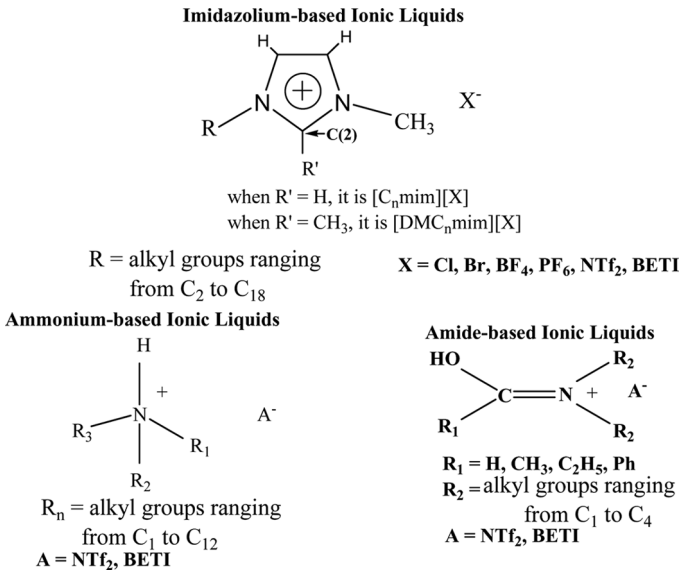

Scheme 1.

their potential applications in gas separation (9). The effect of atmosphere (Nitrogen or air), TGA crucibles, TGA sample mass, and the scan rate on decomposition temperature have also been studied on imidazolium-based ILs (10). In contrast, the thermal stabilities of protic ILs have been investigated at a much less extend. Specifically, Angell and his coworkers have developed a correlation of decomposition temperature with ΔpK_a (12).

EXPERIMENTAL

Materials and Methods

All chemicals and solvents were reagent grade and used without further purification unless noted otherwise. Lithium bis(trifluoromethane sulfonyl) imide (CAS#: 90076-65-6, $LiNTf_2$) and lithium bis(perfluoroethyl sulfonyl) imide (CAS#: 132843-44-8, LiBETI) are purchased from 3M Performance Materials Division. The imidazolium-based ILs were synthesized according to the literature procedures (7). The protocol for synthesizing protic ILs is based on the combination of neutralization and metathesis methodologies (7,13,14). Briefly, organic amines or amides and a slightly excess amount of conc. HCl aqueous solution were mixed at room temperature. The reaction was quite exothermic. To this mixture, either lithium bis(trifluoromethane sulfonyl) imide ($LiNTf_2$) or lithium bis(perfluoroethyl-sulfonyl) imide (LiBETI) pre-dissolved in D.I. water was added in an equal molar ratio. The corresponding IL phase readily formed after the addition of aqueous solution of $LiNTf_2$ or LiBETI. The lower layer (IL phase) was separated from the aqueous phase and washed with D.I. H_2O four times to ensure the removal of LiCl. The final products as nearly colorless free-flowing liquids or solids were dried under vacuum at 70°C for 4 hours.

TGA Measurements

Thermogravimetric analysis curves were measured in nitrogen at a scan rate of 10°C/min with TA instrument TGA 2950.

DSC Measurements

Differential scanning calorimetry curves were performed with a TA instruments DSC Q100. Scanning sequence involves freezing an IL sample to −90°C, maintaining this temperature for 20 min, and then heating the sample to 150°C at 10°C/min.

RESULTS AND DISCUSSIONS

TGA Studies of Selected ILs

(a) TGA of immidazolium-based ILs

The TGA plots of nine dialkylimidazolium bromide ILs and five trialkylimidazolium bromide ILs are compared in Figs. 1 and 2, respectively. As shown from these two figures, the TGA plots of these two classes of bromide ILs are basically overlapped with each other, indicating a very similar thermal behavior. This observation implies that the thermal stability of these two classes of ILs is not strongly dependent on the alkyl chain length on imidazolium cations. Furthermore, the substitution of hydrogen by methyl group in the C(2) position (Scheme 1) of the imidazolium ring has a small effect on the thermal stability of these two classes of ILs. This observed similar thermal stability is consistent with the same decomposition mechanism for these two classes of the ILs. Hofmann elimination has been considered as a key thermal degradation mechanism for imidazolium and ammonium compounds (15).

Figure 3 shows a close comparison of the TGA plots of dialkylimidazolium-bromide ILs {[$C_n$mim][Br]} with those of trialkylimidazolium-bomide ILs {[DMC_nmim][Br]}. If the alkyl chain length is the same, the thermal stabilities of [DMC_nmim][Br] are slightly higher than those of [$C_n$mim][Br]. This observation indicates that the substitution of the C(2) hydrogen with alkyl groups in imidazolium cations increases the

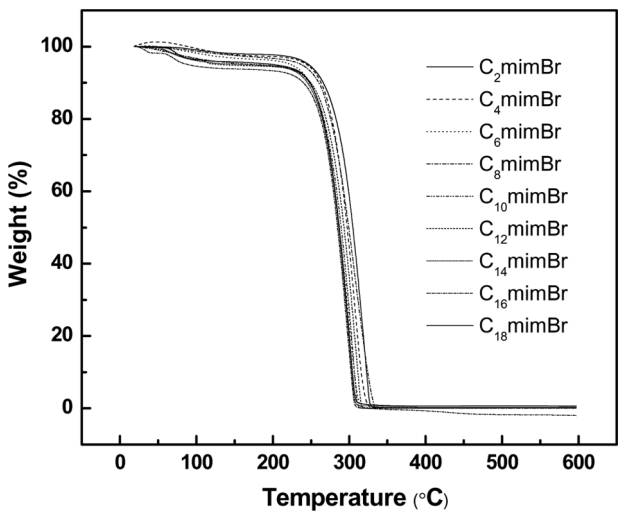

Figure 1. Comparison of TGA plots of Dialkylimidazolium Bromides ILs.

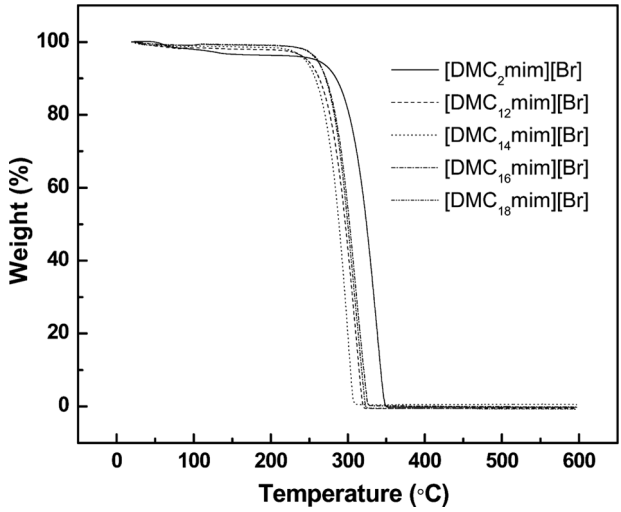

Figure 2. Comparison of TGA plots of Trialkylimidazolium Bromides ILs.

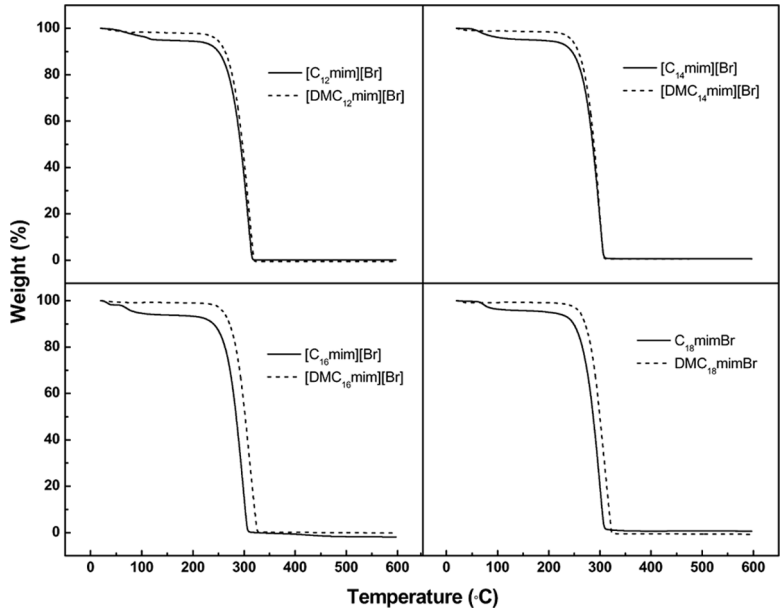

Figure 3. Comparison of TGA plots of Dialkylimidazolium Bromides [$C_n$mim][Br] and Trialkylimidazolim Bromides [DMC_nmim][Br].

Table 1. The T_{onset} (°C) of [$C_n$mim][X]

Anions (X)	[C_2mim][X]	[C_4mim][X]	[C_6mim][X]	[C_8mim][X]
Br	287	279	267	272
BF_4	NM	420	413	411
PF_6	NM	423	361	299
BETI	415	398	401	418
NTf_2	444	421	418	416

thermal stability of the resulting ILs because of the high acidity associated with hydrogen in the C(2) position (16). However, this instability induced by the acidity of hydrogen in C(2) position is relatively small.

As shown in Table 1, the thermal stability of the imidazolium-based ILs strongly depends on the anion of ILs having the same cation. The relative stability observed is: $NTf_2 > BF_4 \approx BETI > PF_6 >> Br$. Except for the ILs having bromide as the conjugate anion, the imidazolium-based ILs are very stable and their onset decomposition temperatures are around 400°C at 10°C/min scan rate. The thermal instability of the bromide ILs is clearly related to the Lewis basicity of Br^-, which facilitates Hofmann elimination (15).

The effect of the TGA sample mass of a specific IL on the TGA plot is illustrated in Fig. 4. As seen from Fig. 4, the increase of the TGA sample mass from 10 mg to 30 mg can lead to an increase of the onset decomposition temperature (T_{onset}) by 10°C at 10°C/min scan rate. Clearly, the interplay of mass transport and evaporation rate plays a small role in determining decomposition temperature. This observation is very interesting and further emphasizes the caution in reporting TGA results.

Figure 5 compares the TGA plots of [DMC_{12}mim][Br] measured at two different heating rates. The decrease in the heating rate by a factor of 10 induced a large decrease (about 40°C) of the onset decomposition temperature. Figures 4 and 5 indicated the typical trends, which have also been observed for other types of ionic liquids. These observations are consistent with what have been reported in literature (10).

(b) TGA of protic ammonium-based ILs

This class of ILs is prepared by proton transfer and therefore classified as protic ILs. As seen from Table 2, the thermal stabilities of this class of protic ILs seem to be essentially independent of the carbon chain length of alkyl groups on ammonium ions. However, there does appear to be a systematic correlation between the anion and the onset decomposition temperature of a specific IL (Fig. 6 and Table 3). For the same

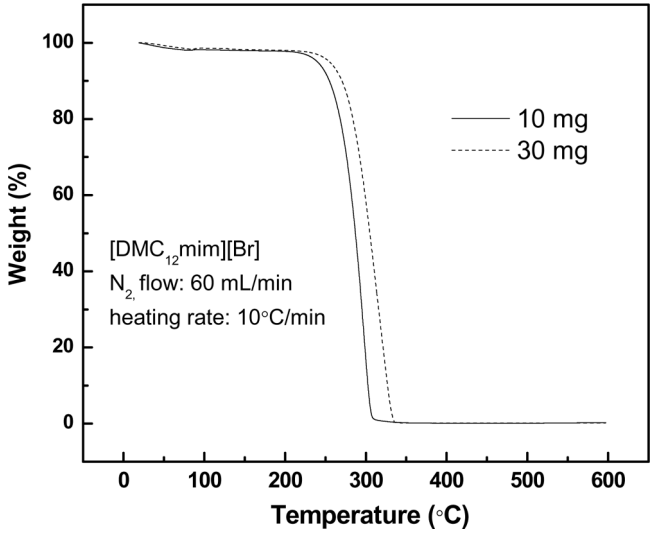

Figure 4. The effect of the sample mass on TGA plots of [DMC_{12}mim][Br].

cation, the ILs with $BETI^-$ as the conjugate anion have slightly lower thermal stabilities (20 degrees lower) than the ILs with NTf_2^- as the conjugate anion. This observation is very interesting, considering the structure and basicity similarities between $BETI^-$ and NTf_2^- (12).

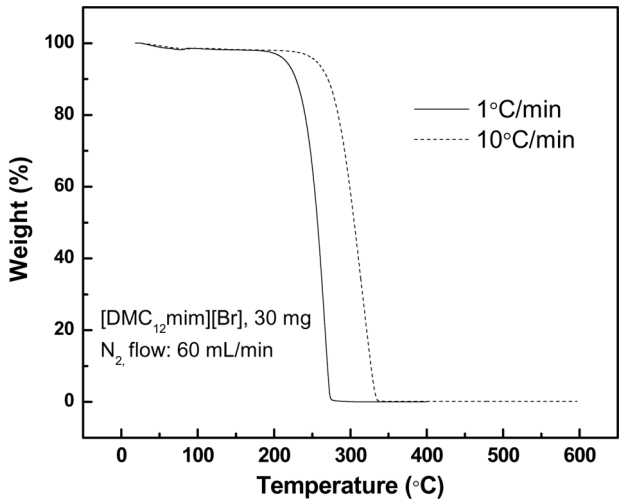

Figure 5. The effect of the heating rate on TGA plots of [DMC_{12}mim][Br].

Table 2. The T_{onset} (°C) of $[(C_nH_{2n+1})_3NH][NTf_2]$

Carbon chain length	C_2	C_3	C_4	C_5	C_6	C_8
$[(C_nH_{2n+1})_3NH][NTf_2]$	360	350	335	340	345	360

Because the ammonium-based ILs may undergo the reverse proton-transfer reaction, these ammonium-based ILs are thermally less stable than imidazolium-based ILs, which have onset decomposition temperatures in the range from 400°C to 440°C as seen in Table 1. As listed in Table 2 and 3, the onset decomposition temperatures for ammonium-based ILs are typically between 300°C and 360°C.

(c) TGA of protic amide-based ILs

The TGA study of amide-based ILs is quite interesting. All ILs based on imidazolium and ammonium cations only undergo an one-step weight loss process as shown in Figs. 1–6. In contrast, TGA curves measured for all sixteen amide-based ILs reveal a two-step weight loss process as shown in Figs. 7 and 8. The calculation of weight balance indicates that the first step is consistent with the loss of the amide of the ILs and the

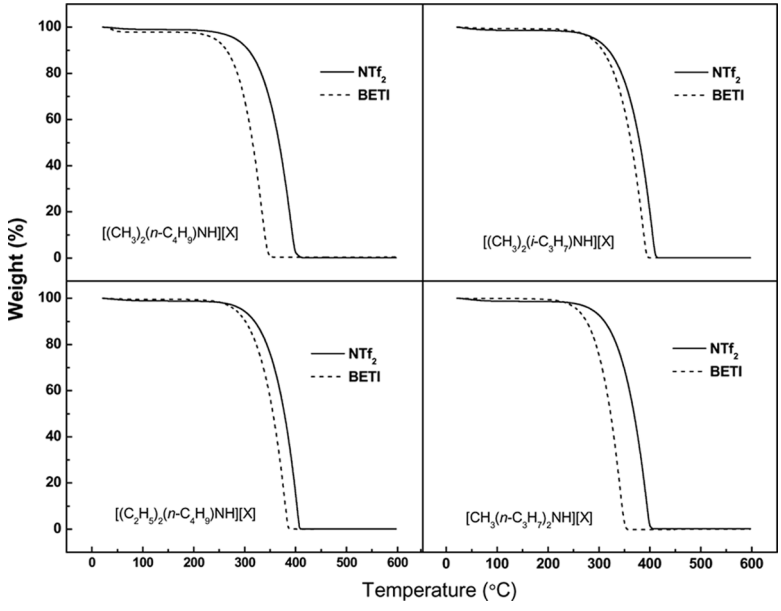

Figure 6. Comparison of TGA plots of ammonium-based ILs $[R_nR'_{3-n}NH][X]$.

Table 3. The T_{onset} (°C) of other ammonium-based ILs

	NTf_2	BETI
$[(CH_3)_2(i\text{-}C_3H_7)NH][X]$	360	340
$[(CH_3)(C_2H_5)_2NH][X]$	360	340
$[(CH_3)_2(n\text{-}C_4H_9)NH][X]$	360	300
$[(CH_3)(n\text{-}C_3H_7)_2NH][X]$	350	300
$[(C_2H_5)_2(n\text{-}C_4H_9)NH][X]$	335	310
$[(i\text{-}C_3H_7)_2(C_2H_5)NH][X]$	350	330
$[(n\text{-}C_8H_{17})NH_3][X]$	350	325

second step is correlated to the loss of the anion of the ILs. The first-step thermal decomposition temperature (T_{onset}) for protonated amide cations is in the range of 180–230°C, about 100°C higher than those of the corresponding free amides. Interestingly, the second-step thermal decomposition temperature (T_{onset}) depends somewhat on the choice of amide cations and roughly lies within a 50°C window centered at 350°C. Again for the same cation, the ILs with NTf_2^- as the conjugate anion have slightly higher thermal stabilities than the ILs with $BETI^-$

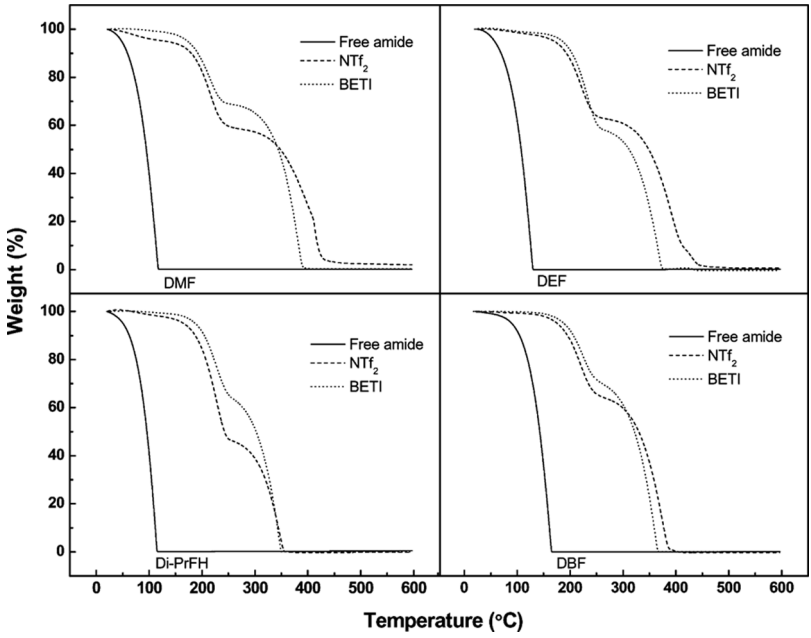

Figure 7. Comparison of TGA plots of amide-based ILs and free amide-1.

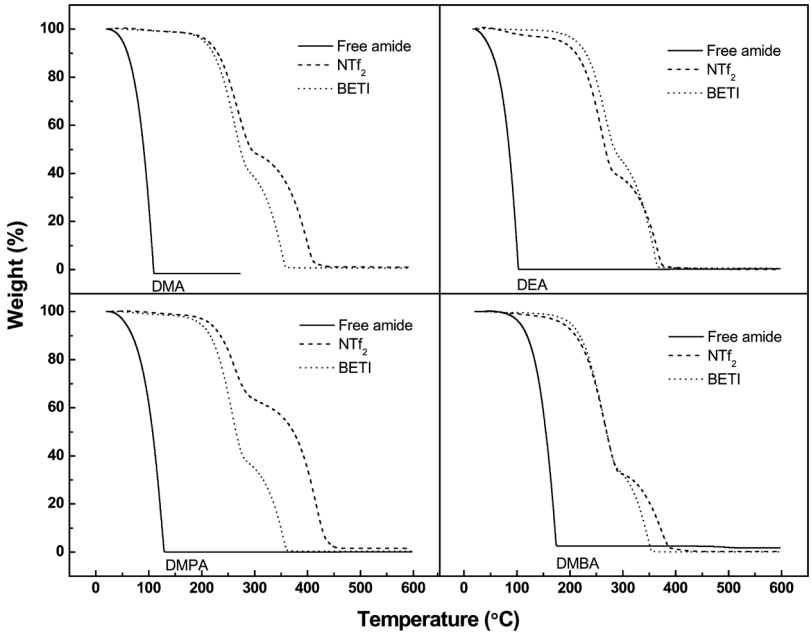

Figure 8. Comparison of TGA plots of amide-based ILs and free amide-2

as the conjugate anion. The difference in $T_{onset}$is closely related to the choice of cations. Generally, larger the substituents on cations are larger differences in $T_{onset}$are.

DSC Studies of Selected ILs

(a) DSC studies of imidazolium-based ILs

As shown in Fig. 9, [$C_n$mim][Br] ILs with a longer carbon chain length ($\geq C_9$) exhibit a sharp heat-absorption peak, which corresponds to the melting point of the corresponding IL. For an example, the DSC curve of [C_{12}mim][Br] shows a sharp phase transition attributed to the melting of a lamellar crystal phase (lower panel of Fig. 9). The sharp phase transition indicates a highly ordered lamellar structure induced by the hydrophobic interaction of alkyl chains and the Coulombic interaction of IL cations and IL anions. As listed in Table 4, the melting points of these imidazolium salts increase with the carbon chain length on the imidazolium ring. However, the DSC plots of [$C_n$mim][Br] with a shorter carbon chain length ($\leq C_8$) do not show any sharp endothermic peak. Both [C_8mim][Br] and [C_6mim][Br] show a tiny peak at

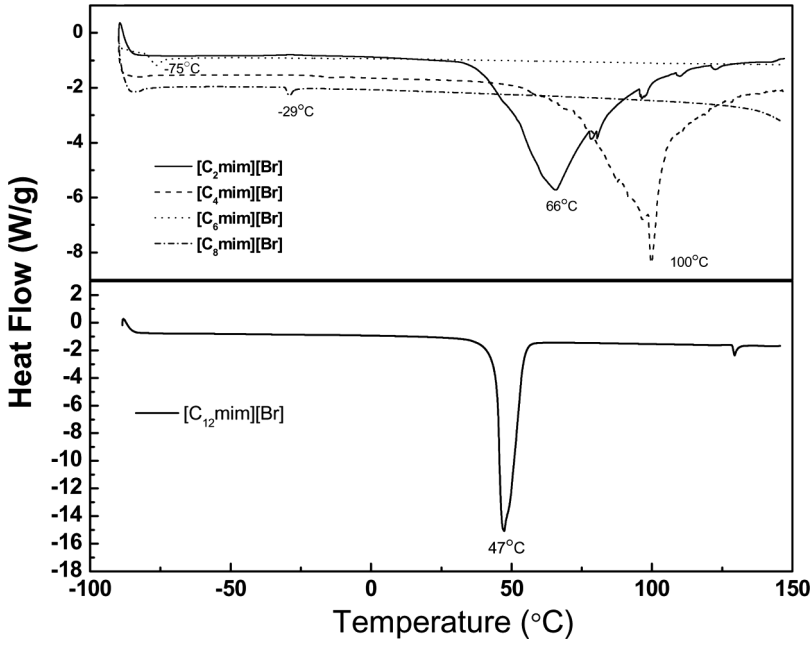

Figure 9. Comparison for DSC plots of Dialkylimidazolium Bromides [$C_n$mim][Br].

$-29^{\circ}C$ and $-75^{\circ}C$, respectively. This observation indicates that the hydrophobic interaction of alkyl chains is very small for [C_8mim][Br] and [C_6mim][Br] to induce lamellar orders because of shorter alkyl chains. Both [C_4mim][Br] and [C_2mim][Br] show a broad peak at $100^{\circ}C$ and $66^{\circ}C$, respectively. This observation indicates that the hydrophobic interaction of alkyl chains is very small but the Coulombic interaction of cations and anions is considerably enhanced because of the short alkyl chain length in these two ILs. The high melting points of these two ILs are attributed to the interplay of strong Coulombic and weak hydrophobic interactions.

The comparison of the DSC plots of [$C_n$mim][Br] with those of [DMC_nmim][Br] is illustrated in Fig. 10. For the same alkyl chain length, the melting point of [$C_n$mim][Br] is about $30^{\circ}C$ lower than that of [DMC_nmim][Br]. This observation indicates that the hydrogen-bonding

Table 4. The heat-absorption temperature (melting point °C) of [$C_n$mim][Br]

Carbon chain length	C_9	C_{10}	C_{12}	C_{14}	C_{16}	C_{18}
[$C_n$mim][Br]	−0.21	30	47	56	65	72

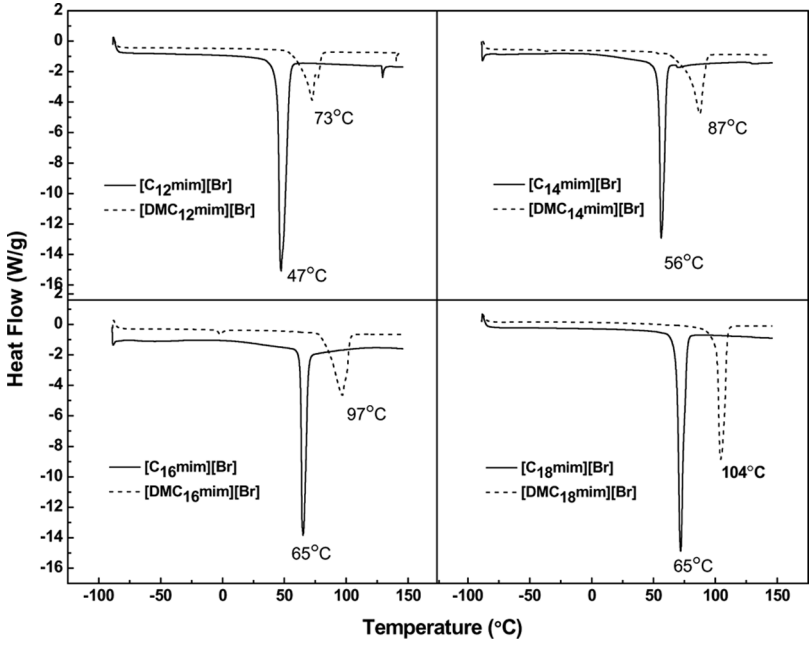

Figure 10. Comparison for DSC plots of Dialkylimidazolium Bromides [$C_n$mim][Br] and Trialkylimidazolim Bromides [DMC_nmim][Br].

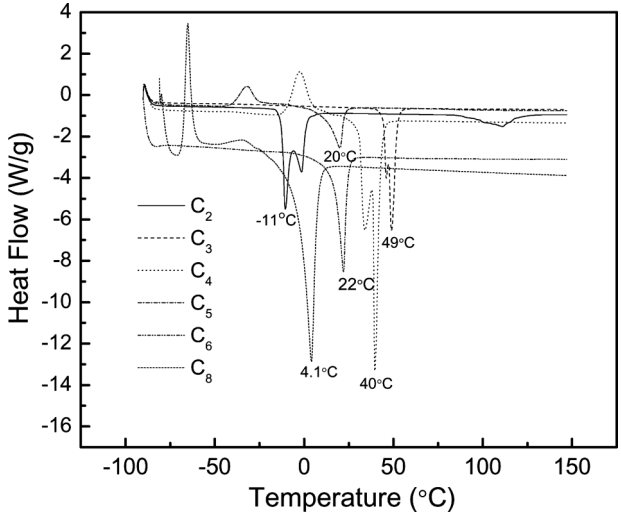

Figure 11. Comparison of DSC plots of Ammonium ILs [(n-C_nH_{2n+1})$_3$ NH][NTf_2].

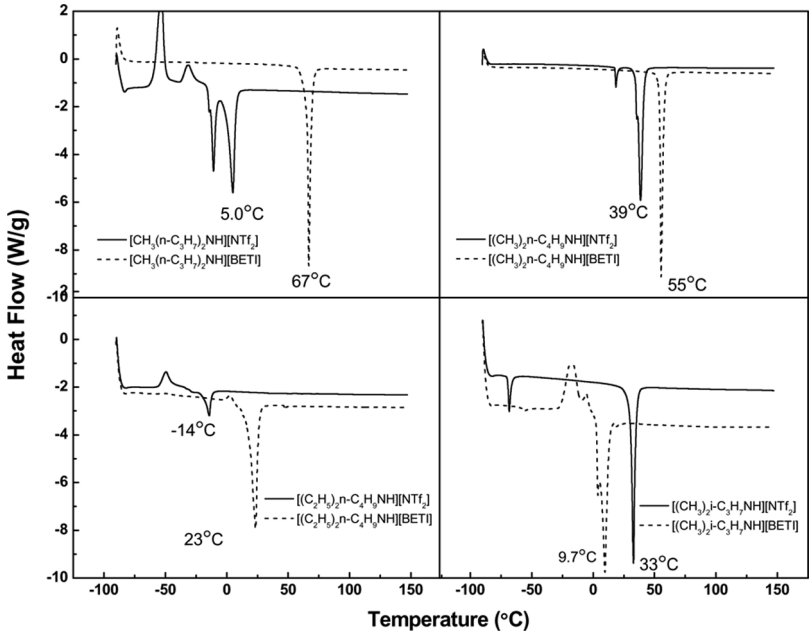

Figure 12. Comparison of DSC plots of ammonium ILs $[R_nR'_{3-n}NH][X]$.

interaction associated with hydrogen in the C(2) position of imidazolium ring is not significant in determining the melting point of a specific imidazolium-based IL. The mass dependence is the key to the determination of melting points for different ILs.

(b) DSC studies of ammonium-based ILs

The DSC plots of the ammonium-based ILs are illustrated in Figs. 11 and 12. For $[(n\text{-}C_nH_{2n+1})_3NH][NTf_2]$ series as shown in Fig. 11 and Table 5, they all give a heat absorption peak, which corresponds to the melting points of the ILs. The melting points are correlated to the alkyl chain length on ammonium cations, which is consistent with the volume-based model. Some of these ILs show an exothermal peak, which

Table 5. The heat-absorption temperature (melting point °C) of $[(C_nH_{2n+1})_3NH][NTf_2]$

Carbon chain length	C_2	C_3	C_4	C_5	C_6	C_8
$[(C_nH_{2n+1})_3NH][NTf_2]$	−11	49	40	20	22	4.1

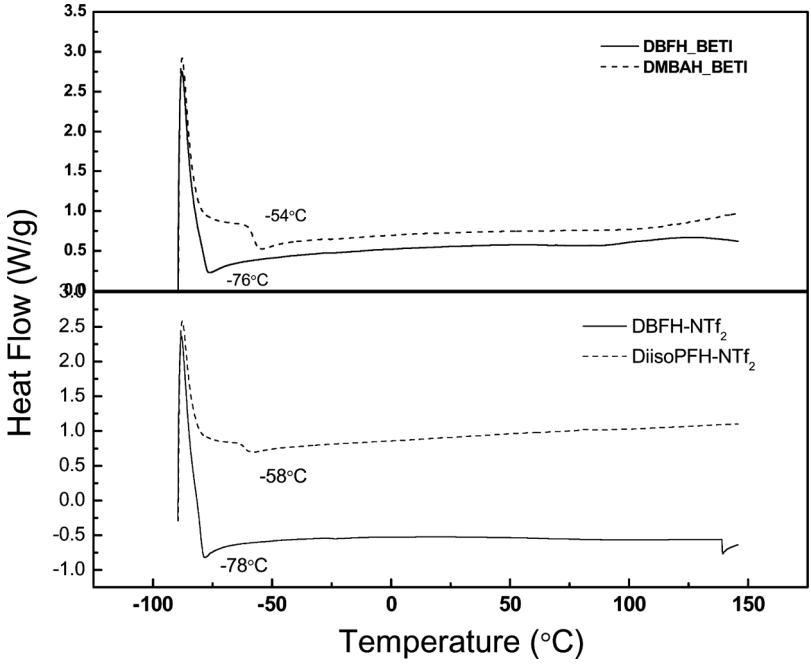

Figure 13. Comparison of DSC plots of amide-based ILs.

could be assigned to the crystallization point. Most of these ILs do not have any glass transition peak. As shown in Fig. 12, for the same cation, the ILs with NTf^- as the conjugate anion have the heat absorption peak at lower temperature than the ILs with $BETI^-$ as the conjugate anion. This observation is consistent with the volume-based thermodynamic model (17,18).

(c) DSC studies of amide-based ILs

Unlike the above two classes of ILs, the DSC plots of amide-based ILs do not give much information as shown in Fig.13. Some of them have a broad peak in the range of $-80^\circ C$ to $-50^\circ C$, which could be assigned to the corresponding glass-transition points. The lack of any endothermic peak associated with melting indicates that these protic ILs are highly disordered.

CONCLUSIONS

We have systematically investigated the thermal properties of aprotic imidazolium-based, protic ammonium-based, and protic amide-based

ILs by TGA and DSC. The variation of thermal stabilities and melting points as function of IL structural properties was systematically studied. The dependence of phase transitions on IL structures was also studied through DSC measurement. These thermal stability data are valuable in designing new separation, catalysis, and energy storage systems based on ILs.

ACKNOWLEDGMENT

This research was supported by the Environmental Management Science Program of the Office of Science and Environmental Management, U.S. Department of Energy, under Contract DE-AC05–0096OR22725 with Oak Ridge National Laboratory, managed by UT-Battelle, LLC. Sheng Dai would like to thank Basic Energy Sciences, U.S. Department of Energy, under Contract DE-AC05–0096OR22725 with Oak Ridge National Laboratory for financial support.

REFERENCES

1. Welton, T. (1999) Room-temperature ionic liquids. Solvents for synthesis and catalysis. *Chem. Rev.*, *99*: 2071.
2. Wasserscheid, P.; Keim, W. (2000) Ionic liquids—New "solutions" for transition metal catalysis. *Angew. Chem. Int. Ed.*, *39*: 3773.
3. Rogers, R. D.; Seddon, K. R. (2003) Ionic liquids—Solvents of the future? *Science*, *302*: 792.
4. Dai, S.; Ju, Y. H.; Barnes, C. E. (1999) Solvent extraction of strontium nitrate by a crown ether using room-temperature ionic liquids. *J. Chem. Soc. Dalton Trans.*, 1201.
5. Luo, H. M.; Dai, S.; Bonnesen, P. V. (2004) Solvent extraction of Sr^{2+} and Cs^{+} based on room-temperature ionic liquids containing monoaza-substituted crown ethers. *Anal. Chem.*, *76*: 2773.
6. Luo, H. M.; Dai, S.; Bonnesen, P. V.; Buchanan, A. C.; Holbrey, J. D.; Bridges, N. J.; Rogers, R. D. (2004) Extraction of cesium ions from aqueous solutions using calix[4]arene-bis(tert-octylbenzo-crown-6) in ionic liquids. *Anal. Chem.*, *76*: 3078.
7. Bonhote, P.; Dias, A. P.; Papageorgiou, N.; Kalyanasundaram, K.; Gratzel, M. (1996) Hydrophobic, highly conductive ambient-temperature molten salts. *Inorg. Chem.*, *35*: 1168.
8. Ngo, H. L.; LeCompte, K.; Hargens, L.; McEwen, A. B. (2000) Thermal properties of imidazolium ionic liquids. *Thermochim. Acta*, *357*: 97.
9. Fredlake, C. P.; Crosthwaite, J. M.; Hert, D. G.; Aki, S.; Brennecke, J. F. (2004) Thermophysical properties of imidazolium-based ionic liquids. *J. Chem. Eng. Data*, *49*: 954.

10. Kosmulski, M.; Gustafsson, J.; Rosenholm, J. B. (2004) Thermal stability of low temperature ionic liquids revisited. *Thermochim. Acta*, *412*: 47.
11. Van Valkenburg, M. E.; Vaughn, R. L.; Williams, M.; Wilkes, J. S. (2005) Thermochemistry of ionic liquid heat-transfer fluids. *Thermochim. Acta*, *425*: 181.
12. Yoshizawa, M.; Xu, W.; Angell, C. A. (2003) Ionic liquids by proton transfer: Vapor pressure, conductivity, and the relevance of Delta pK(a) from aqueous solutions. *J. Am. Chem. Soc.*, *125*: 15411.
13. Huang, J. F.; Luo, H. M.; Liang, C. D.; Sun, I. W.; Baker, G. A.; Dai, S. (2005) Hydrophobic bronsted acid-base ionic liquids based on PAMAM dendrimers with high proton conductivity and blue photoluminescence. *J. Am. Chem. Soc.*, *127*: 12784.
14. Luo, H. M.; Yu, M.; Dai, S. (2007) Solvent extraction of Sr^{2+} and Cs^{+} based on hydrophobic protic ionic liquids. *Z. Naturfors. Sect. A-J. Phys. Sci.*, *62*: 281.
15. Hine, J. (1962) *Physical Organic Chemistry;* McGraw-Hill: New York.
16. Dai, S.; Shin, Y. S.; Toth, L. M.; Barnes, C. E. (1997) Comparative UV-Vis studies of uranyl chloride complex in two basic ambient-temperature melt systems: The observation of spectral and thermodynamic variations induced via hydrogen bonding. *Inorg. Chem.*, *36*: 4900.
17. Glasser, L.; Jenkins, H. D. B. (2005) Predictive thermodynamics for condensed phases. *Chem. Soc. Rev.*, *34*: 866.
18. Glasser, L. (2004) Lattice and phase transition thermodynamics of ionic liquids. *Thermochim. Acta*, *421*: 87.